acta medica

ORIGINAL ARTICLE

Comparison of two main fragmentation methods of amyloid beta fibrils for establishing an Alzheimer disease model in cell culture

Elham Bahador Zırh[1]
ORCID: 0000-0002-6921-2365

Hare Yazgı[2]
ORCID: 0009-0001-3818-4576

Hilal Akyel[3,4]
ORCID: 0000-0003-2841-6668

Cahide Banu Tel[4]
ORCID: 0000-0001-5453-1294

Selim Zırh[5]
ORCID: 0000-0002-7962-6078

[1] Department of Histology and Embryology, Faculty of Medicine, TOBB Economy and Technology University, Ankara, Türkiye

[2] Department of Neurology, Faculty of Medicine, Ankara University, Ankara, Türkiye

[3] Department of Pharmacology, Faculty of Pharmacy, Başkent University, Ankara, Türkiye

[4] Department of Pharmacology, Faculty of Pharmacy, Hacettepe University, Ankara, Türkiye

[5] Department of Histology and Embryology, Faculty of Medicine, Erzincan Binali Yıldırım University, Erzincan, Türkiye

Corresponding Author: Selim Zırh
E-mail: szirh@erzincan.edu.tr

Received: 3 January 2025, Accepted: 14 April 2025, Published online: 20 June 2025

ABSTRACT

Aim: Amyloid beta fibrils have been shown to play a role in plaque formation and aggregation in Alzheimer's disease. Obtaining these fibrils using two main methods and applying them to Alzheimer's modelling is crucial in understanding the pathology of the disease at the molecular level and identify in therapeutic targets. The aim of our study is to determine the optimum sonication parameters using probe and ultrasonic bath sonication laboratory methods and to demonstrate Alzheimer's disease modelling at the cellular level.

Methods: Lyophilized human peptide amyloid beta$_{1-42}$ fibrils (fAβ_{1-42}) were subjected to probe sonication for 1 minute with 1, 3 and 5 second on/off pulse applications at varying ambient temperatures (room temperature, ice and ice surrounded by dry ice [ISDI]) for 20, 40 and 60 cycles, respectively. Then, ultrasonic bath sonication was performed in 10 °C water for 1 hour. The length of the fragmented fibrils was quantified by transmission electron microscopy (TEM). fAβ_{1-42} at different concentrations was applied to SH-SY5Y cell line. The non-toxic dose and time of fAβ_{1-42} application were analysed using the WST-1 assay. Intracellular and extracellular fibrils were visualized with immunofluorescence (IF) labelling.

Results: Although, fragmentation was observed under all conditions, it was observed that fibrillar lengths decreased as the on/off pulse times increased, regardless of the number of cycles with ice and dry ice. Additionally, decreasing the temperature increased fibrillar fragmentation.

Conclusion: We anticipate that our study will contribute to the literature by developing an effective and economical sonication method for fibrillar fragmentation with two main laboratory methods and obtaining fAβ_{1-42} that can be used in cells at optimum concentration.

Keywords: Amyloid beta, Alzheimer disease, sonication method, fragmentation, SH-SY5Y

INTRODUCTION

Amyloidosis is a broad term that encompasses various protein misfolding diseases, all characterized by the accumulation of soluble precursor proteins into insoluble aggregates outside the cell. It is known that this fibrillar structure, which is unbranched and has a diameter of approximately 10 nm, generally has non-parallel peptides that form a beta-pleated structure [1]. In the pathology of Alzheimer's disease (AD), amyloid beta (Aβ) peptides, produced through the breakdown of amyloid precursor protein (APP), play a significant role as they aggregate to form amyloid plaques [2]. Although the main cause of AD - characterized by dementia, memory problems and learning difficulties due to the neuron damage - [3], is not yet fully understood, it has been stated that Aβ plaques

can accumulate outside the nerve cells and disrupt the signalling transmission between them, leading to functional losses such as memory impairment as a result of brain damage [4]. Furthermore, this accumulation has been suggested to trigger immunity by causing neuroinflammation [5].

The significance of Aβ oligomer internalization in the pathogenesis of AD has been demonstrated in numerous studies. One study provided evidence that the uptake of oligomers via pinocytosis increases neurotoxicity, while a reduction in toxicity induction is observed in the absence of intracellular uptake [6]. Additionally, research has shown that inhibiting endocytosis prevents neuronal damage, suggesting that intracellular amyloid beta$_{1-42}$ (Aβ$_{1-42}$) plays a more critical role in neurodegeneration than extracellular aggregates [7]. Another study indicated that intracellular Aβ impairs intracellular trafficking and organelle movement, potentially contributing to synaptic damage [8]. Furthermore, Aβ oligomer internalization has been shown to potentiate tau pathology, leading to increased synaptic toxicity [9]. Consequently, preventing Aβ oligomer internalization has been emphasized as a potential therapeutic target in AD research.

The APP, a type 1 transmembrane structure, is encoded by the *APP* gene located on human chromosome 21 [10-12]. This protein, which is particularly expressed in the central nervous system and has a role in various physiological processes, consists of 639-770 amino acids [13]. The processing of APP into smaller fragments, including the ~4 kDa Aβ peptide [14], is carried out by three key secretases: α-secretase, β-secretase, and γ-secretase [15]. In amyloidogenic and non-amyloidogenic pathways involving these secretases, the soluble APP domain is generated through the combined action of α- and γ- secretase [15], while the insoluble Aβ$_{1-42}$ form is produced via the cooperation of β-secretase and γ-secretase [16]. During plaque formation, Aβ$_{1-40}$ and Aβ$_{1-42}$ forms are the main components. With the increase in the Aβ$_{1-42}$/Aβ$_{1-40}$ ratio in favour of Aβ$_{1-42}$, this structure, promotes protein misfolding, forms protein aggregates and plaques [2], causing toxicity for cells. These plaques stimulate immune system cells and cause inflammation, which further contributing to damage to neurons [16].

In addition to the frequent use of animal models to study human diseases, their evolutionary differences may affect the accuracy of scientific findings [17]. *In vitro* methods offer significant advantages for investigating tau and amyloid pathology, analysing biochemical products and organelles, testing therapeutic agents, and understanding AD, as they better represent the natural microenvironment of the pathology [18]. Both *in vitro* and *in vivo* studies have demonstrated that high molecular weight oligomers, known as protofibrils, not only increase amyloid plaque aggregation but also contribute to neuronal degeneration and cognitive impairment [19]. It has been reported that utilizing these methods is beneficial for gaining a deeper understanding of the disease mechanism and exploring potential solutions. Specifically, they provide valuable insights into the structural intermediates and fibrils formed during the aggregation process, starting from high-yield recombinant Aβ peptide and its oligomeric building blocks [20].

In addition to the fact that the sonication method has been shown to promote Aβ aggregation [21], it has also been observed that proteins associated with the disease or not associated with the disease form amyloid during sonication [22]. Changes in the covalent bond structure of proteins, along with factors such as high temperature, elevated pH levels, or alcohol addition, can disrupt protein stabilization and promote amyloid aggregation *in vitro*. Sonication contributes to amyloid pathology, which stimulates immunity in the living organism and leads to disease, by disrupting protein stabilization [21]. Transmission electron microscopy (TEM) can be employed to assess the length and diameter of fibrils obtained post-sonication, verifying through imaging whether small fibrils of homogeneous size are produced [23]. However, evidence suggests that molecular conformation and aggregation potential have a greater impact on neurotoxicity than size characteristics [24].

In this study, fibril fragmentation was achieved using both probe and ultrasonic bath sonication methods. Probe sonication involved 20, 40, and 60 cycles under varying pulse durations (1, 3, and 5 seconds on/off) and ambient temperatures (room temperature (RT), ice, and ice surrounded by dry ice [ISDI]). In terms of probe sonication, a pulse duration of 1 second on/off is most commonly used, while RT is the preferred ambient temperature [25,26]. To evaluate a range of pulse durations, we chose 1, 3, and 5 seconds on/off. Although RT is the

most preferred ambient, some studies use ice for sonication [24,27], so we included both conditions for comparison. Additionally, we surrounded the ice with dry ice to further cool the environment, preventing re-fibrillation due to heating and assessing whether more effective fragmentation could be achieved. Moreover, [24] reported the sonication of fibrils for 20 cycles, whereas [28] indicated that fibrils were sonicated for 60 cycles. Therefore, we applied 20, 40 and 60 cycles to determine the optimal sonication cycle. The primary aim was to evaluate the effects of 20, 40, and 60 cycles of probe sonication on fibril fragmentation while maintaining constant pulse durations and ambient temperatures. Additionally, fibrils were subjected to bath sonication for 1 hour at 10 °C, as described by Creed et al. [29], aiming to compare the effects of probe sonication and ultrasonic bath sonication on $A\beta_{1-42}$ fragmentation. Following TEM verification, the immunofluorescence technique was employed to determine whether fibrils associated with AD pathology could be observed in the presence of cells. Thereby, an AD cell model was subsequently established.

MATERIALS AND METHODS

Preparation of Amyloid Beta$_{1-42}$ Fibrils (fAβ_{1-42})

$A\beta_{1-42}$ human peptide (lyophilized-1 mg) were purchased from Peptiteam, Middle East Technical University, Ankara, Turkiye.

$A\beta_{1-42}$ is reported to spontaneously form amyloid fibrils upon incubation of $A\beta_{1-42}$ solution at 37 °C at a concentration that is much higher than the physiological concentration of its in biological fluids [30]. Additionally, it is widely known oligomeric $A\beta_{1-42}$ intermediates, which are denoted fibrillar oligomers, enter the fibril-forming pathway to form fibrils [31]. In order to form fAβ_{1-42}, $A\beta_{1-42}$ peptide was dissolved in 1,1,1,3,3,3-hexafluoro-2-propanol (HFIP) and dried overnight under laminar flow cabinet. The peptide microfilm was then dissolved in sterile phosphate buffer salin (PBS) (200 µM, pH 7.4). The unaggregated peptide was incubated at 37 °C for 24 h, and then gently mixed to promote aggregation. Next, fAβ_{1-42} was aliquoted and stored -20 °C until it will be used [32] (Table 1).

Sonication of fAβ_{1-42}

Sonications were performed with a probe sonicator and an ultrasonic bath sonicator. Sonication steps were conducted in a biosafety level-2 cabinet in order to prevent exposure to fibrils that may become aerosolized during probe sonication (Figure 1).

Probe Sonication

1. Attach a 3 mm diameter probe to the converter, and set the general sonicator parameters (30% amplitude; the time to 0:01:00). The amplitude value of 30% [33] and a duration of 1 minute were the most commonly used in previous studies [25,26] was also selected for our study. Pulse duration, sonication cycles and ambient temperature were set as stated in Table 2.

2. Thaw fibrils at room temperature (RT) ($24^0C \pm 2$).

3. To achieve a final concentration (20 µM), stock solution of fAβ_{1-42} was diluted with sterile-filtered deionized water (dH_2O) or PBS to 200 µl volume for TEM imaging or cell culture experiments, respectively.

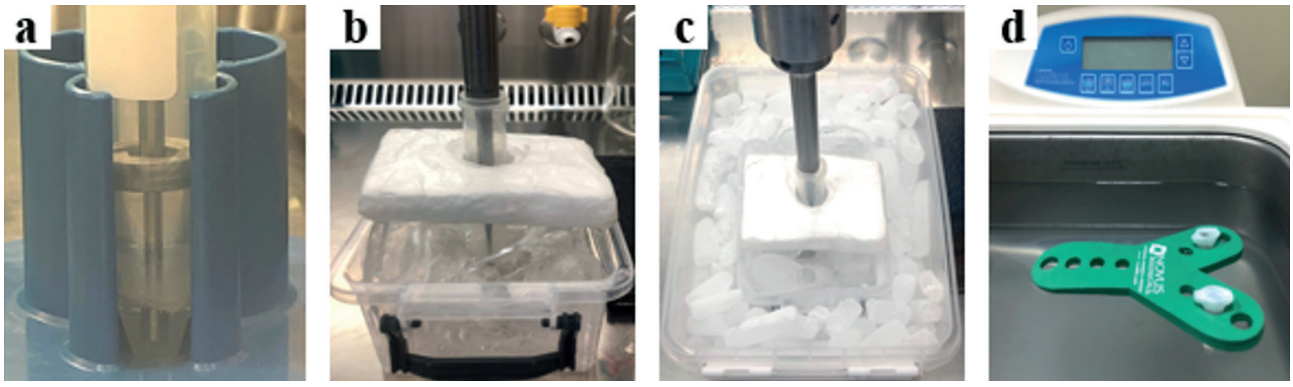

Figure 1. Sonication Images. Probe sonication at RT (a), in ice (b), in ISDI (c), ultrasonic bath sonication (d).

Table 1. Materials used in all experiments

Name	Company	Catalog Number
Antibodies		
Beta Amyloid 1-42 Polyclonal Antibody	Bioss	BS-0107R
Goat Anti-Rabbit IgG H&L (Alexa Fluor® 488)	Abcam	ab150077
Cell Line		
Human Neuroblastoma Cells (SH-SY5Y)	ATCC	CRL-2266
Equipments		
Steril Conical Centrifuge Tubes, 15 ml	Greiner Bio-One, Cellstar®	
Steril Conical Centrifuge Tubes, 50 ml	Greiner Bio-One, Cellstar®	
Steril Microcentrifuge Tube, 1.5 ml	Greiner Bio-One, Cellstar®	
Parafilm	Parafilm M	PM-996
Stopper	Made in our laboratory	
Lockable Tweezer		
Formvar/Carbon Coated Copper Grids	Ted Pella Inc.	01801
Grids Box	Ted Pella Inc.	
Cell Culture Flask, 75 cm^2	Greiner Bio-One, Cellstar®	658175
Cell Culture Chamber Slide	SPL Life Sciences	30108
Devices		
Centrifuge Device	Hitachi	Himac CT6E
Probe Sonicator	Sonics Vibra-Cell™	VCX 750
Probe	Sonics Vibra-Cell™	630–0422 (microtip)
Utrasonic Bath Sonicator	Branson	CPX5800H
Transmission Electron Microscope	FEI	Tecnai G^2 Spirit BioTwin model
Microplate Reader	Heales	MB-580 Elisa Reader
Fluorescent Microscope	Leica	DM 2000 LED
Proteins		
Human Amyloid Beta1-42	Purchased from Peptiteam, Ankara, Turkiye	
Reagents		
1,1,1,3,3,3-Hexafluoro-2-propanol (HFIP)	Sigma-Aldrich	105228-5G
Uranyl Acetate	Eletron Microscopy Sciences	22400
Dulbecco's Modified Eagle Medium (DMEM)	Capricorn Scientific	DMEM-HA
L-Glutamine	Capricorn Scientific	GLN-B
Penicillin–Streptomycin	Capricorn Scientific	PS-B
Fetal Bovine Serum	Capricorn Scientific	FBS-HI-22A
Trypsine-EDTA	Capricorn Scientific	TRY-3B
WST-1	Roche	Cellpro-Ro-11 644 807 001
Phosphate-Buffer Salin	Capricorn Scientific	PBS-1A
Normal Goat Serum	Capricorn Scientific	GOA-1B
EPI-IHC-Antibody Diluent	EpiplasT	D220520-100 ml
UltraCruz® Aqueous Mounting Medium with DAPI	Santa Cruz Biotechnology	sc-24941-10 ml

4. The probe was cleaned using 70% ethanol and sterile distilled water. Additionally, the probe was sterilized with UV light for 15 minutes.

5. In order to minimize the loss of fibrils, a parafilm-wrapped stopper with a hole was placed inside the sterile conical centrifuge tube (15 ml).

6. Place the probe tip in the middle of the sample.

a. It is important that the probe tip does not touch either the tube or the stopper in order to prevent energy loss.

b. In order to prevent shifting during sonications in ice (-20^{0}C ± 4) and in ISDI (-80^{0}C ± 10), a white foam holder was placed around the sterile conical centrifuge tube.

Table 2. Probe and ultrasonic bath sonication protocols for fibrils

Sonication Technique	Sonication Features		
	Cycles	Pulse (on/off)	Temperature
Probe	20 / 40 / 60	1 second / 1 second	-Room temperature (240C ± 2)
		3 second / 3 second	-Ice (-200C ± 4)
		5 second / 5 second	-Ice surrounded by dry ice (-800C ± 10)
Ultrasonic Bath	1 hour		10 °C (water temperature)

7. Move the probe up and down during each pulse to ensure that all fibrils are sonicated.

8. To prevent the tube from overheating, wait one minute between each 1-minute sonication cycle.

9. In order to collect liquid that splashes onto walls, remove the probe from the sample and briefly centrifuge it at 2000 g for 1 second.

10. Following that, the entire volume was transferred to a sterilized microcentrifuge tube.

11. To clean the probe, wipe it with lab tissue dampened with 1% SDS, 70% ethanol, and distilled water, respectively. Then, dry the probe with a lab tissue.

12. Detach the probe from the converter and store.

13. After cleaning the cabinet with 1% SDS, wipe it down with 70% ethanol.

a. The 1% SDS solution was used to dissociate fibrils and clean surfaces and equipments.

Ultrasonic Bath Sonication

1. The temperature of the distilled water was set to 10°C in the bath tank.

2. The entire sample volume (200 µl) was immersed in water using a holder.

3. Sonication was performed for one hour.

Transmission Electron Microscopy for $fA\beta_{1-42}$ Visualization

The bench surface was covered with a parafilm. Copper grids (200 mesh, Ted Pella Inc.), coated with formvar and carbon, were washed twice on the drops of deionized water (dH_2O) for one minute each time. After washing, the grids were gently blotted with filter paper. The grids were then floated on a drop of $fA\beta_{1-42}$ sample for 3 minutes and blotted again with filter paper. Next, the grids were negatively stained by applying two 1% (w/v) uranyl acetate drops for one minute each and filtered to remove excess uranyl acetate. Afterward, was removed by wicking with filter paper. Finally, the grids were stored in a grid box until imaging. The TEM images were taken by the Central Laboratory at Middle East Technical University, Ankara, Turkiye, using a Tecnai G^2 Spirit BioTwin TEM (FEI) at 65,000× magnification. The grids were examined at a magnification of 65000 using a TEM (Tecnai G^2 Spirit BioTwin, FEI). The microscope was equipped with a LaB6 gun operated at an acceleration voltage of 80 kV. Fibril lengths were measured using ImageJ 1.53k software for semi-quantitative analysis [34,35].

Cell Culture

Human neuroblastoma cells (SH-SY5Y) were obtained from the American Type Culture Collection (ATCC, Manassas, VA, USA). Cells were cultured in Dulbecco's modified Eagle's medium (DMEM)-high glucose supplemented with 10% foetal bovine serum (FBS), 2 mM L-glutamine, 100 U/mL penicillin/streptomycin. Cells were maintained in T75 flasks at 37 °C in a 5% CO_2 atmosphere. Cells from passage 2 were used in the experiments. For assays, cells were plated on 96-well plates or 8-well chamber slides and grown to 70–80% confluence [36].

Assessment of $A\beta_{1-42}$ Administration by WST-1 Assay

Cell viability following $A\beta_{1-42}$ treatment was assessed using the WST-1 assay (Roche, Cat no 11 644 807 001) to determine the optimal concentration of Aβ and treatment time for inducing Aβ pathology. SH-SY5Y cells were seeded at 4×10^3 cells/well in 96-well plates with 200 µL growth medium [37].

After 24 hours, the cells were treated with different concentrations of $A\beta_{1-42}$. Samples of $A\beta_{1-42}$ was diluted with the growth medium to prepare serial concentrations (1 µM, 5 µM, 10 µM, 20 µM; [38,39]). At hours 24 and 48 after $A\beta_{1-42}$ treatment, 10 µL of WST-1 solution was added to the each well and incubated for 4 hours. Absorbance was measured at 450–600 nm using a microplate reader (Heales, MB-580 Elisa Reader, India), and cell viability was calculated. Each concentration and time point was tested in triplicate [37].

Immunofluorescence Staining for SH-SY5Y Cells

For immunofluorescence, SH-SY5Y cells were cultured on 8-well chamber slides. After fixation with 100% methanol for 5 minutes, cells were washed with PBS. Serum blocking was performed using 1:50 goat serum for 1 hour. The primary antibody (bs-0107R, $A\beta_{1-42}$ Polyclonal Antibody, Bioss, USA, 1:200) was incubated with cells at room temperature for 2h. After washing with PBS, cells were incubated with seconder antibody (ab150077, Abcam, USA, 1:1000) in the dark and RT conditions for 1h. Nuclei were stained with DAPI (H-2000, Vector Laboratories, USA). The slides were analyzed using a fluorescent microscope. In 400X magnification, micrographs were captured and analyzed.

Statistical Analysis

TEM data were expressed as mean ± standard error of the mean (SEM) and analyzed using GraphPad Prism Version 7.0 (GraphPad Software Inc., San Diego, CA). The normality of the experimental data was assessed using the Shapiro–Wilk test. For comparisons between multiple groups, one-way ANOVA followed by Dunnett's multiple comparisons test was applied for normally distributed data, while the Kruskal-Wallis test followed by Dunn's multiple comparisons test was used for non-normally distributed data. For comparison of two groups (ultrasonic bath analysis), the Mann-Whitney test was employed. A p-value < 0.05 was considered statistically significant.

RESULTS

Transmission Electron Microscopy for $fA\beta_{1-42}$ Visualization

In our study, we aimed to expose Aβ fibrils to different sonication conditions (20, 40 and 60 cycles with probe sonication and ultrasonic bath) and various ambient temperatures (RT, in ice, and in ISDI) to fragment the fibrils to the required for cellular uptake and AD model formation. To assess the efficacy of these methods, we measured the fibril length using TEM and calculated the mean length.

When evaluating probe sonication parameters, a statistically significant reduction in fibril length was observed in all groups compared to the control. Notably, the extension of the pulse time led to successful fibril fragmentation, irrespective of the ambient temperature and number of cycles. Among these results, fibrils were significantly broken in all on/off pulse groups compared to the control group in the groups with 20, 40 and 60 cycles (Table 2). As the on/off pulse duration increased from 1 second to 3 and 5 seconds, fibril fragment lengths decreased (Table 3, Figure 2, 3, 4 and 5).

Fibrils must be shorter than 100 nm to internalize into cells and induce intracellular neuropathology [40,41]. Accordingly, among the probe sonication methods tested, the average length measurements of fibrils after the following treatments were all below 100 nm: 20 cycles with 5 second on/off pulse at ice (mean length: 86.97±4.653 nm), 40 cycles with 5 second on/off pulse at RT, and 40 cycles with 5 second on/off pulse in ISDI (mean lengths: 89.93±5.988 nm and 96.79±9.662 nm, respectively); 60 cycles with 5 second on/off pulse at RT, and 60 cycles with 5 second on/off pulse in ISDI (mean lengths: 96.64±3.09 nm and 98.93±7.298 nm, respectively). The average fibril length obtained from ultrasonic bath sonication (mean length: 92.62±2.755 nm) also fell below 100 nm (Table 3, Figure 2, 3, 4 and 5). These results demonstrate that decreasing the temperature and extending the on/off pulse duration in probe sonication significantly enhance fibril fragmentation.

Table 3. Mean of fibrillar lengths of all groups

20 CYCLES – 100 nm Room Temperature (RT)				
	Control	**1 sec on/off**	**3 sec on/off**	**5 sec on/off**
Mean	386.8	259.6	208.9	183.5
SEM	19.66	5.871	11.04	8.808
Ice				
	Control	**1 sec on/off**	**3 sec on/off**	**5 sec on/off**
Mean	386.8	215.7	198.9	186.92
SEM	19.66	11.69	12.17	4.653
Ice surrounded by dry ice				
	Control	**1 sec on/off**	**3 sec on/off**	**5 sec on/off**
Mean	386.8	202.1	177.4	141.7
SEM	19.66	8.857	13.66	7.63
40 CYCLES – 100 nm RT				
	Control	**1 sec on/off**	**3 sec on/off**	**5 sec on/off**
Mean	386.8	221.9	193.4	89.93
SEM	19.66	9.571	9.759	5.988
Ice				
	Control	**1 sec on/off**	**3 sec on/off**	**5 sec on/off**
Mean	386.8	226.7	200.5	136.2
SEM	19.66	6.503	15.89	10.18
Ice surrounded by dry ice				
	Control	**1 sec on/off**	**3 sec on/off**	**5 sec on/off**
Mean	386.8	221.2	153.5	96.79
SEM	19.66	11.52	9.52	9.662
60 CYCLES – 100 nm RT				
	Control	**1 sec on/off**	**3 sec on/off**	**5 sec on/off**
Mean	386.8	215.6	170.3	96.64
SEM	19.66	13.5	13.51	3.09
Ice				
	Control	**1 sec on/off**	**3 sec on/off**	**5 sec on/off**
Mean	386.8	198	160.6	148.8
SEM	19.66	5.766	12.25	8.645
Ice surrounded by dry ice				
	Control	**1 sec on/off**	**3 sec on/off**	**5 sec on/off**
Mean	386.8	119.4	149.2	98.93
SEM	19.66	9.292	13.26	7.298
ULTRASONIC BATH – 100 nm				
	Control		**Bath**	
Mean	386.8		92.62	
SEM	19.66		2.755	

All values are nanometers (SEM: standard error of the mean).

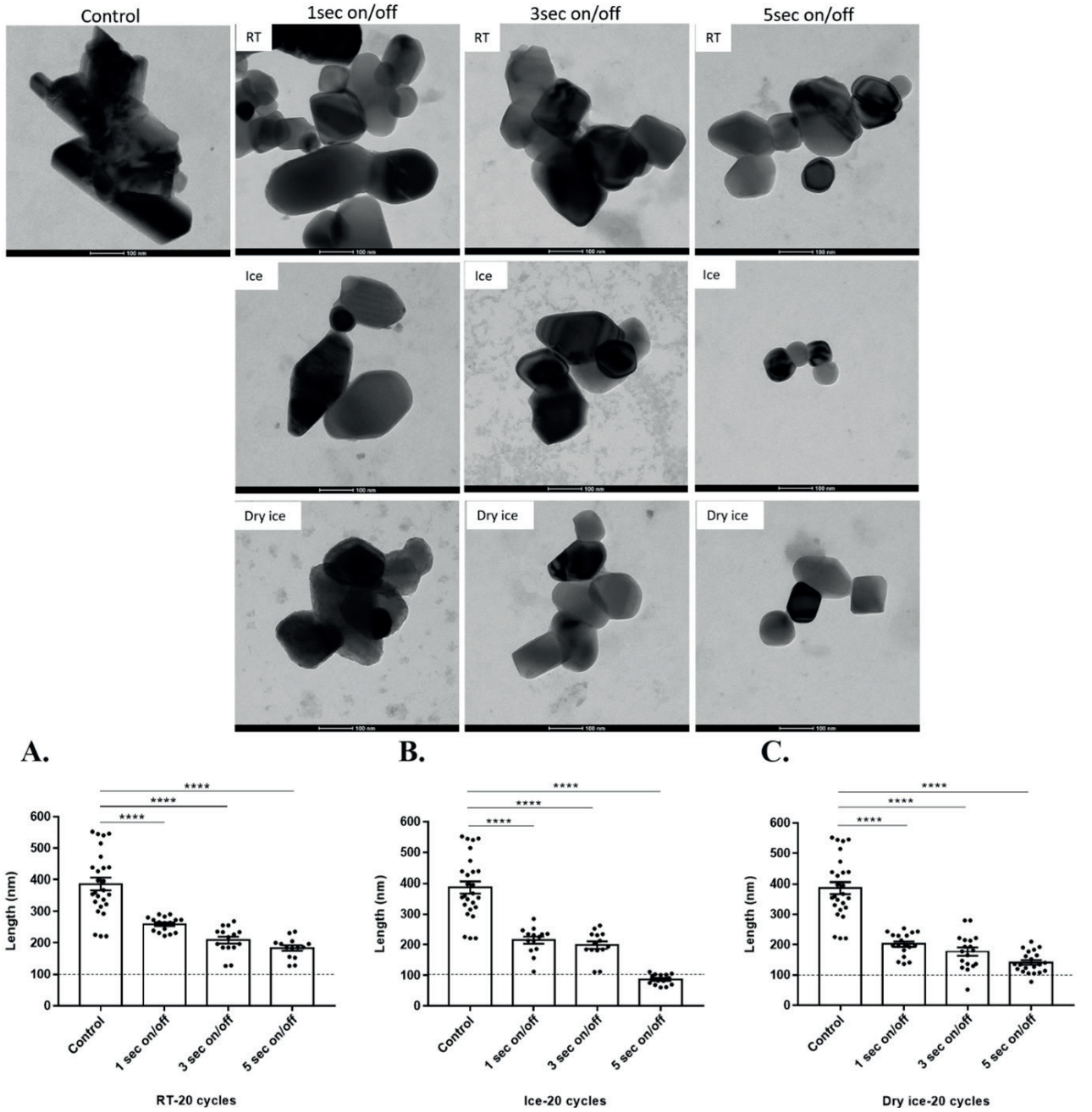

Figure 2. Changes in fAβ1-42 length, following 20 cycles probe sonication in different temperature and pulse duration.

The fibrils were significantly broken in all pulse groups compared to control group (A) at RT (****p=0.0001; one-way ANOVA followed by post hoc Dunnett's multiple comparisons test), (B) in ice (****p=0.0001; one-way ANOVA followed by post hoc Dunnett's multiple comparisons test), and (C) in ISDI (****p=0.0001; one-way ANOVA followed by post hoc Dunnett's multiple comparisons test, scale bars are 100 nm).

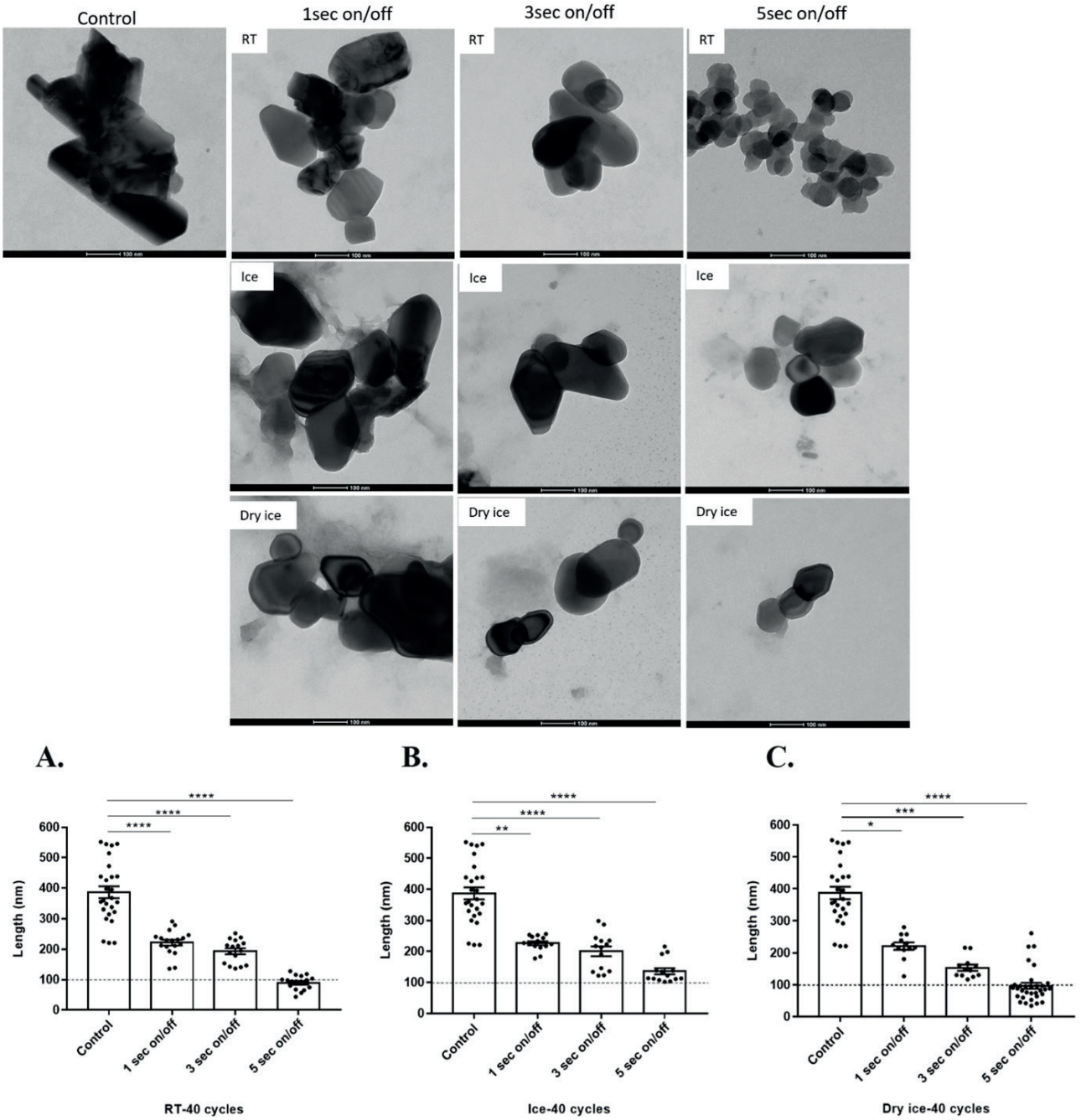

Figure 3. Changes in fAβ_{1-42} length, following 40 cycles sonication in different temperature and pulse duration.

The fibrils were significantly broken in all pulse groups compared to control group (A) at RT (****p=0.0001; one-way ANOVA followed by post hoc Dunnett's multiple comparisons test), (B) in ice (**p=0.0023; ****p<0.0001, Kruskal Wallis followed by post hoc Dunn's multiple comparisons test), and (C) in ISDI. (*p=0.0424, ***p=0.0002, ****p<0.0001; Kruskal Wallis followed by post hoc Dunn's multiple comparisons test, scale bars are 100 nm).

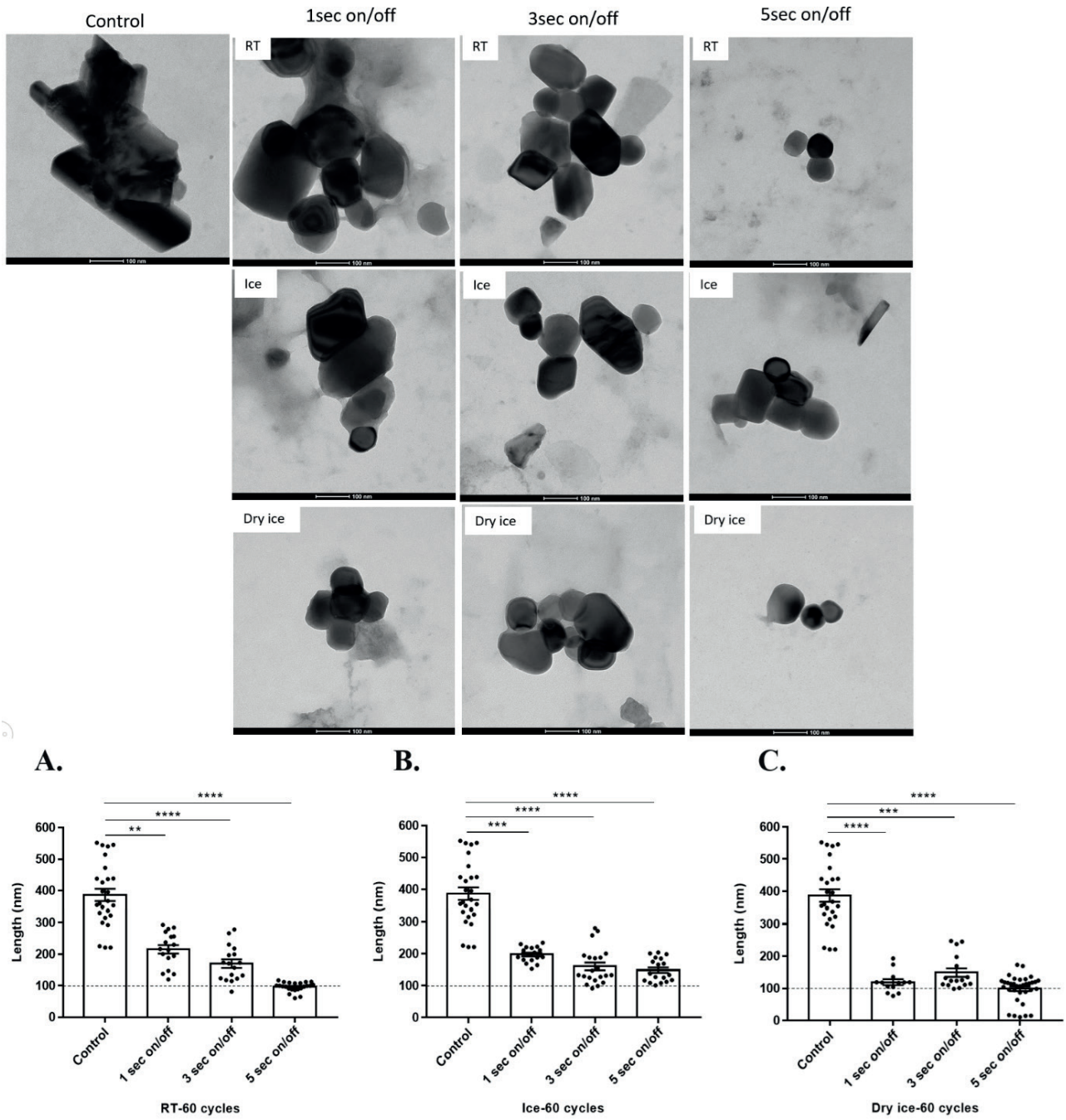

Figure 4. Changes in fAβ_{1-42} length, following 60 cycles sonication in different temperature and pulse duration.

The fibrils were significantly broken in all pulse groups compared to control group (A) at RT (**p=0.0058, ****p<0.0001; Kruskal Wallis followed by post hoc Dunn's multiple comparisons test), (B) in ice (***p=0.0005; ****p<0.0001, Kruskal Wallis followed by post hoc Dunn's multiple comparisons test), and (C) in ISDI. (***p=0.0002, ****p<0.0001; Kruskal Wallis followed by post hoc Dunn's multiple comparisons test, scale bars are 100 nm).

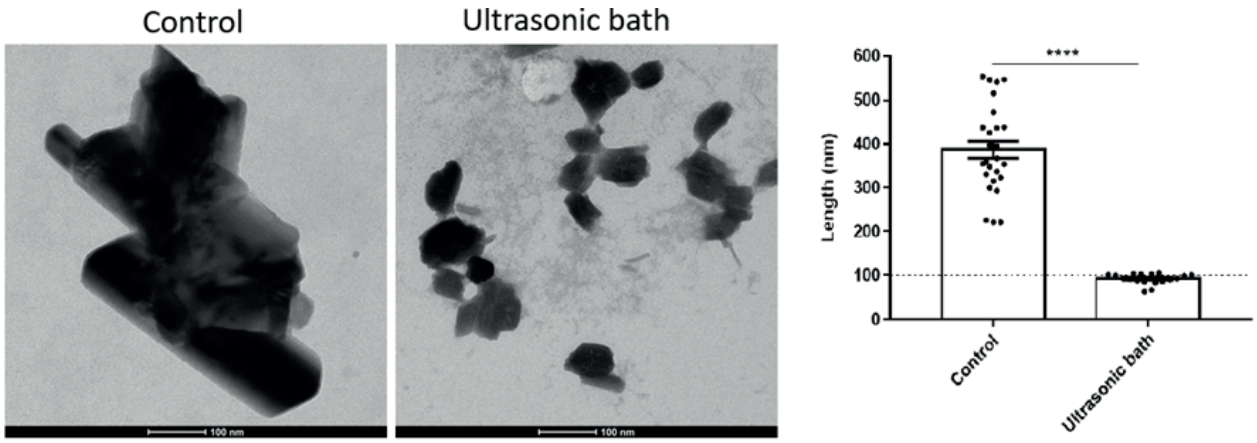

Figure 5. Changes in $fA\beta_{1-42}$ length, following ultrasonic bath sonication.

The fibrils were significantly broken in ultrasonic bath group compared to control group (****p<0.0001; Mann Whitney test, scale bars are 100 nm).

A

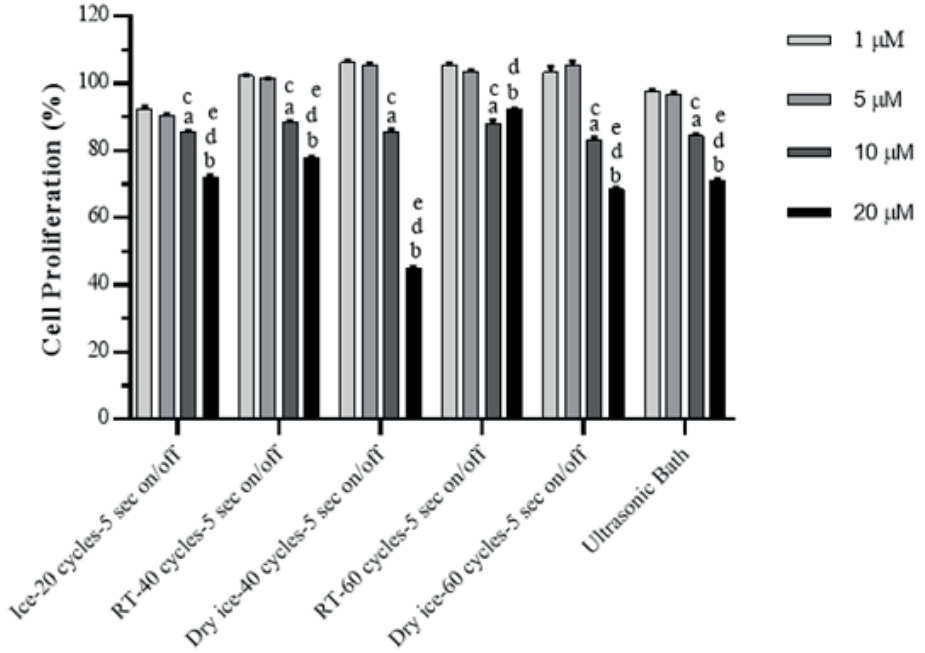

B

	1 µM		5 µM		10 µM		20 µM	
Sonication	**Mean**	**SEM**	**Mean**	**SEM**	**Mean**	**SEM**	**Mean**	**SEM**
1	92.430	0.840	90.368	0.570	85.732	0.344	72.077	0.681
2	102.353	0.164	101.527	0.132	88.575	0.320	77.756	0.478
3	106.137	0.784	105.383	0.617	85.534	0.927	45.115	0.364
4	105.316	0.781	103.673	0.359	88.164	1.020	92.487	0.118
5	103.311	1.795	105.476	1.184	83.211	0.847	68.549	0.541
6	97.825	0.462	96.707	0.736	84.545	0.525	70.973	0.594

Figure 6. A: The percentage of cell proliferation after administration with different concentrations of selected sonication species at 48 hours. **B:** Sonication species: 1: Ice-20 cycles-5 second on/off; 2: RT-40 cycles-5 second on/off; 3: Dry-ice-40 cycles-5 second on/off; 4: RT-60 cycles-5 second on/off; 5: Dry ice-60 cycles-5 second on/off; 6: Ultrasonic Bath.

Data are presented as percentages of the control group. Data was given as mean ± SEM of three replicates of experiments. Different letters show statistically significant differences between concentrations in all groups (a p<0.0001 1 µM vs 10 µM; b p<0.0001 1 µM vs 20 µM; c p<0.05 5 µM vs 10 µM; d p<0.0001 5 µM vs 20 µM; e p<0.0001 10 µM vs 20 µM; two-way ANOVA followed by post hoc Tukey).

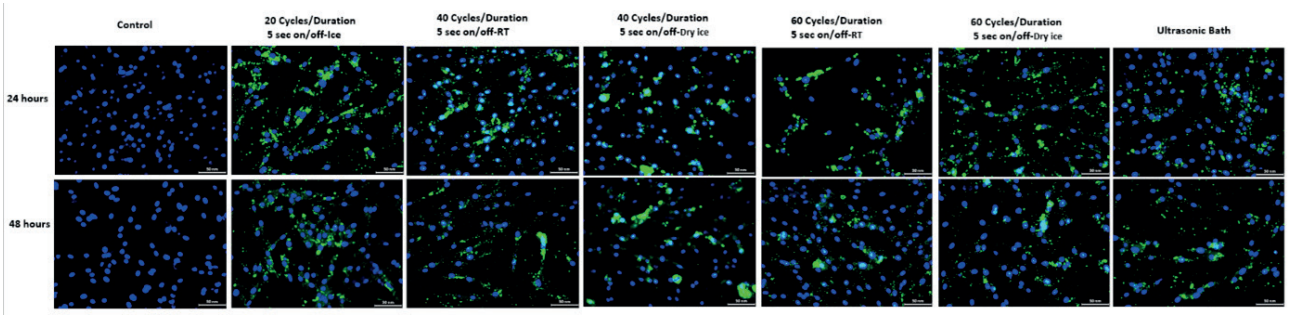

Figure 7. Immunofluorescence staining of all groups.

$A\beta_{1-42}$ accumulations were seen on both intracellular and extracellular areas. As indicated in the reference papers [54,55], images were captured at x40 magnification (Blue: nuclei, green: $A\beta_{1-42}$ protein; scale bars are 50 nm).

Assessment of $A\beta_{1-42}$ Administration by WST-1 Assay

To determine the optimal non-toxic concentration of Aβ fibrils for in vitro application, we employed the colorimetric WST-1 assay. Fibrils with an average length below 100 nm (produced by ice-20 cycles-5 second on/off; RT-40 cycles-5 second on/off; dry-ice-40 cycles-5 second on/off; RT-60 cycles-5 second on/off; dry-ice-60 cycles-5 second on/off; and ultrasonic bath methods) were administered to SH-SY5Y cells at 1, 5, 10, and 20 µM concentrations. Based on the results, 5 µM was identified as the highest non-toxic dose (Figure 6).

Immunofluorescence Staining for SH-SY5Y Cells

To visualize the accumulation of broken Aβ fibrils in SH-SY5Y cells, indirect immunofluorescence was performed. Cells were incubated with fibrils at a 5 µM concentration for 24 and 48 hours. Both intracellular and extracellular accumulation of Aβ fibrils was observed in each group, with a notable increase in accumulation at 48 hours compared to 24 hours (Figure 7).

DISCUSSION

Aβ accumulation is a hallmark of neuroinflammation and cell death in AD [42]. This accumulation disrupts neuronal signalling and contributes to the progression of AD pathology [4]. Understanding the behaviour of Aβ in both *in vivo* and *in vitro* models is critical for identifying potential therapeutic targets [43]. In our study, we compared different sonication methods to find the most effective procedure for fragmenting Aβ fibrils for AD model creation. Our findings indicate that varying the pulse durations (1, 3, and 5 seconds) during sonication significantly contributes to fibril fragmentation. Moreover, performing sonication at lower temperatures (ice or ISDI) enhanced fibril breakdown. Sonication, both with probe and ultrasonic bath methods, has been shown to be effective for producing sufficiently fragmented Aβ fibrils that can be used for AD [21,44].

The aggregation tendency of the fragments obtained by preserving the structural properties of the protein through the sonication method applied to mature fibrils is important for the formation of a realistic model [24]. It has been stated that acoustic cavitations occur with both probe and ultrasonic bath sonication, which are performed to provide a homogeneous distribution and fragmentation within the fibrils. It has been stated that an increase in the duration and power of the mentioned sonication methods reduces the stability of the liquids containing nanoparticles and that there is an optimum point for thermal conductivity [45]. One of the aims of our study was to evaluate the effect of 1-minute sonication performed for 20, 40 or 60 cycles. To prevent protein denaturation during sonication, a 1-minute rest period was applied between each 1-minute sonication cycle. After sonication, TEM imaging was used to observe amyloid fibril morphology and for measuring the length of the fibrils [46]. When the decrease of the fibril lengths in the repeat groups were compared with the control group, it was revealed that the extension of the sonication time was statistically significant, independent of the ambient temperature and the number of cycles. These data are also consistent with previous studies [23]. It was also observed that the lengths of the formed fibril fragments decreased as the on/off times increased, regardless of the number of cycles. The duration of the pulses exerted an effect on the fragmentation of amyloid fibrils. This suggests that different pulse durations may cause changes in the fragmentation of fibrils. Consequently, this study aimed to investigate the effect of different pulse durations

(1, 3 and 5 seconds on/off) on the fragmentation of fibrils. According to TEM images, the findings show that the on/off pulses increasing from 1 second to 3 and 5 seconds, regardless of the number of pulses (20-40 and 60 repetitions), decreased the lengths of fibrils. The working principle of sonication is to create acoustic cavitation and create intense zones of shear with extreme pressure and heat. While it has been stated that Aβ formation can be triggered in these regions at ambient temperatures [44], another study has also reported that accumulation increases with temperature at below the thermal denaturation point (60 ^{0}C) in sonication-induced aggregation and then decreases when the temperature is further increased [21]. In our study, experiments were conducted at RT and in different ice environments. It was observed that fibrils broke in all environments during sonication. The average fibril length showed a proportional decrease in accordance with the decrease in ambient temperature. According to our findings, decreasing the temperature and extending the on/off time increase the breaking success of Aβ fibrils.

The use of *in vitro* assays is important for drug screening because it reduces the use of animals and provides advantages in initial risk screening [47]. Analyses are possible with various cells in which Aβ accumulation can be observed in precursor or mature form [48,49]. Besides, these fibrils were observed in both intracellular and extracellular areas of SH-SY5Y cells and resulted in a time-dependent increase in total Aβ aggregation.

An immunofluorescence analysis of total amyloid density showed that lyophilized human peptide $A\beta_{1-42}$ fibrils were formed by SH-SY5Y cells after 24 and 48 hours of incubation. When reviewing the literature, it has been seen that in similar studies on drug targets in AD models created with the same cell group, the incubation period is generally applied as 24 and 48 hours [36,50-52]. Following this, in these studies intra and extracellular $A\beta_{1-42}$ accumulation was visualized by immunofluorescence. Our results successfully established the pathological image of fragmented fibrils in both spaces produced by different sonication procedures following incubations.

We propose that the sonication methods and the variable parameters utilized in this study may serve as an optimization framework to enhance the diversity of methodologies in the literature for developing AD models. Furthermore, we anticipate that this model, designed for drug targeting applications, will provide a valuable contribution to the existing body of knowledge.

Strengths

Our study provides a comprehensive examination of the sonication parameters that can be used to generate fragmented $fA\beta_{1-42}$ for the creation of an AD cell model. It presents, for the first time, a comparison between probe and ultrasonic bath sonication methods and investigates the impact of different parameters in probe sonication. Moreover, our study makes a significant contribution to the development of a reproducible and cost-effective sonication protocol for $fA\beta_{1-42}$ under diverse laboratory conditions.

Limitations

Although the durations of ultrasonic bath sonication varied in previous studies [23,27], we selected a single duration based on our specifications of ultrasonic bath sonicator. Additionally, while different forms of $A\beta_{1-42}$ are generated under varying incubation times, this study specifically focused on the sonication of $A\beta_{1-42}$ fibrils under a single incubation time, however, different incubation durations could potentially affect the fibril structure [24,25,53].

Author contribution

Study conception and design: EBZ, HY and SZ; data collection: EBZ, HA and SZ; analysis and interpretation of results: EBZ, HA and SZ; draft manuscript preparation: EBZ, HY, HA, CBT and SZ. All authors reviewed the results and approved the final version of the manuscript.

Ethical approval

The study was approved by the Hacettepe University Local Ethics Committee for Animal Experiments (Protocol no. 2023/03-06, April 11, 2023). This methods article represents the first phase of the broader research project.

Funding

The authors declare that the study received no funding.

Conflict of interest

The authors declare that there is no conflict of interest.

REFERENCES

[1] Hazenberg BPC. Amyloidosis: A clinical overview. Rheum Dis Clin North Am 2013;39(2):323-345. https://doi.org/10.1016/j.rdc.2013.02.012

[2] Ferrari C, Sorbi S. The complexity of Alzheimer's disease: An evolving puzzle. Physiol Rev 2021;101(3):1047-1081. https://doi.org/10.1152/physrev.00015.2020

[3] Geldmacher DS, Whitehouse PJ. Evaluation of dementia. N Engl J Med 1996;335(5):330-336. https://doi.org/10.1056/NEJM199608013350507

[4] Salehi A, Delcroix JD, Swaab DF. Alzheimer's disease and NGF signaling. J Neural Transm (Vienna) 2004;111(3):323-345. https://doi.org/10.1007/s00702-003-0091-x

[5] Sigurdsson EM, Knudsen E, Asuni A, et al. An attenuated immune response is sufficient to enhance cognition in an Alzheimer's disease mouse model immunized with amyloid-beta derivatives. J Neurosci 2004;24(28):6277-82. https://doi.org/10.1523/JNEUROSCI.1344-04.2004

[6] Nazere K, Takahashi T, Hara N, et al. Amyloid beta is internalized via macropinocytosis, an HSPG- and lipid raft-dependent and rac1-mediated process. Front Mol Neurosci 2022;15:804702. https://doi.org/10.3389/fnmol.2022.804702

[7] Yu C, Nwabuisi-Heath E, Laxton K, Ladu MJ. Endocytic pathways mediating oligomeric Abeta42 neurotoxicity. Mol Neurodegener 2010;5:19. https://doi.org/10.1186/1750-1326-5-19

[8] Umeda T, Ramser EM, Yamashita M, et al. Intracellular amyloid β oligomers impair organelle transport and induce dendritic spine loss in primary neurons. Acta Neuropathol Commun 2015;3:51. https://doi.org/10.1186/s40478-015-0230-2

[9] Kadamangudi S, Marcatti M, Zhang WR, et al. Amyloid-β oligomers increase the binding and internalization of tau oligomers in human synapses. Acta Neuropathol 2024;149(1):2. https://doi.org/10.1007/s00401-024-02839-2

[10] Goldgaber D, Lerman MI, McBride OW, Saffiotti U, Gajdusek DC. Characterization and chromosomal localization of a cDNA encoding brain amyloid of Alzheimer's disease. Science 1987;235(4791):877-880. https://doi.org/10.1126/science.3810169

[11] Yoshikai S, Sasaki H, Doh-ura K, Furuya H, Sakaki Y. Genomic organization of the human amyloid beta-protein precursor gene. Gene 1990;87(2):257-263. https://doi.org/10.1016/0378-1119(90)90310-n

[12] Lamb BT, Sisodia SS, Lawler AM, et al. Introduction and expression of the 400 kilobase amyloid precursor protein gene in transgenic mice [corrected]. Nat Genet 1993;5(1):22-30. https://doi.org/10.1038/ng0993-22

[13] Müller UC, Zheng H. Physiological functions of APP family proteins. Cold Spring Harb Perspect Med 2012;2(2):a006288. https://doi.org/10.1101/cshperspect.a006288

[14] Masters CL, Multhaup G, Simms G, Pottgiesser J, Martins RN, Beyreuther K. Neuronal origin of a cerebral amyloid: Neurofibrillary tangles of Alzheimer's disease contain the same protein as the amyloid of plaque cores and blood vessels. EMBO J 1985;4(11):2757-2763. https://doi.org/10.1002/j.1460-2075.1985.tb04000.x

[15] Orobets KS, Karamyshev AL. Amyloid precursor protein and alzheimer's disease. Int J Mol Sci 2023;24(19):14794. https://doi.org/10.3390/ijms241914794

[16] Awasthi M, Singh S, Pandey VP, Dwivedi UN. Alzheimer's disease: An overview of amyloid beta dependent pathogenesis and its therapeutic implications along with in silico approaches emphasizing the role of natural products. J Neurol Sci 2016;361:256-271. https://doi.org/10.1016/j.jns.2016.01.008

[17] Pinals RL, Tsai LH. Building in vitro models of the brain to understand the role of APOE in Alzheimer's disease. Life Sci Alliance 2022;5(11):e202201542. https://doi.org/10.26508/lsa.202201542

[18] Ranjan VD, Qiu L, Tan EK, Zeng L, Zhang Y. Modelling Alzheimer's disease: Insights from in vivo to in vitro three-dimensional culture platforms. J Tissue Eng Regen Med 2018;12(9):1944-1958. https://doi.org/10.1002/term.2728

[19] Ono K, Tsuji M. Protofibrils of amyloid-β are important targets of a disease-modifying approach for Alzheimer's disease. Int J Mol Sci 2020;21(3):952. https://doi.org/10.3390/ijms21030952

[20] Chhetri G, Pandey T, Chinta R, Kumar A, Tripathi T. An improved method for high-level soluble expression and purification of recombinant amyloid-beta peptide for in vitro studies. Protein Expr Purif 2015;114:71-76. https://doi.org/10.1016/j.pep.2015.05.015

[21] Stathopulos PB, Scholz GA, Hwang YM, Rumfeldt JAO, Lepock JR, Meiering EM. Sonication of proteins causes formation of aggregates that resemble amyloid. Protein Sci 2004;13(11):3017-3027. https://doi.org/10.1110/ps.04831804

[22] Stefani M, Dobson CM. Protein aggregation and aggregate toxicity: New insights into protein folding, misfolding diseases and biological evolution. J Mol Med (Berl) 2003;81(11):678-699. https://doi.org/10.1007/s00109-003-0464-5

[23] Abrao-Nemeir I, Meyer N, Nouvel A, et al. Aβ42 fibril and non-fibril oligomers characterization using a nanopipette. Biophys Chem 2023;300:107076. https://doi.org/10.1016/j.bpc.2023.107076

[24] Vadukul DM, Maina M, Franklin H, Nardecchia A, Serpell LC, Marshall KE. Internalisation and toxicity of amyloid-β 1-42 are influenced by its conformation and assembly state rather than size. FEBS Lett 2020;594(21):3490-3503. https://doi.org/10.1002/1873-3468.13919

[25] Beretta C, Svensson E, Dakhel A, et al. Amyloid-β deposits in human astrocytes contain truncated and highly resistant proteoforms. Mol Cell Neurosci 2024;128:103916. https://doi.org/10.1016/j.mcn.2024.103916

[26] Konstantinidis E, Dakhel A, Beretta C, Erlandsson A. Long-term effects of amyloid-beta deposits in human iPSC-derived astrocytes. Mol Cell Neurosci 2023;125:103839. https://doi.org/10.1016/j.mcn.2023.103839

[27] Zhang T, Wu J, Wang Y, Zhang H, Zhan X. Alleviating neuronal inflammation induced by Aβ42 in SH-SY5Y through interaction with polysialic acid-oligomannuronate conjugate. Int J Biol Macromol 2024;276(Pt 1):133862. https://doi.org/10.1016/j.ijbiomac.2024.133862

[28] Redmann M, Wani WY, Volpicelli-Daley L, Darley-Usmar V, Zhang J. Trehalose does not improve neuronal survival on exposure to alpha-synuclein pre-formed fibrils. Redox Biol 2017;11:429-437. https://doi.org/10.1016/j.redox.2016.12.032

[29] Creed RB, Memon AA, Komaragiri SP, Barodia SK, Goldberg MS. Analysis of hemisphere-dependent effects of unilateral intrastriatal injection of α-synuclein pre-formed fibrils on mitochondrial protein levels, dynamics, and function. Acta Neuropathol Commun 2022;10(1):78. https://doi.org/10.1186/s40478-022-01374-z

[30] Kakio A, Yano Y, Takai D, et al. Interaction between amyloid beta-protein aggregates and membranes. J Pept Sci 2004;10(10):612-621. https://doi.org/10.1002/psc.570

[31] Huang YR, Liu RT. The toxicity and polymorphism of β-amyloid oligomers. Int J Mol Sci 2020;21(12):4477. https://doi.org/10.3390/ijms21124477

[32] Kasza Á, Penke B, Frank Z, et al. Studies for improving a rat model of Alzheimer's disease: Icv administration of well-characterized β-amyloid 1-42 oligomers induce dysfunction in spatial memory. Molecules 2017;22(11):2007. https://doi.org/10.3390/molecules22112007

[33] Patterson JR, Polinski NK, Duffy MF, et al. Generation of alpha-synuclein preformed fibrils from monomers and use in vivo. J Vis Exp 2019;148. https://doi.org/10.3791/59758

[34] Schmitz M, Candelise N, Canaslan S, et al. α-Synuclein conformers reveal link to clinical heterogeneity of α-synucleinopathies. Transl Neurodegener 2023;12(1):12. https://doi.org/10.1186/s40035-023-00342-4

[35] Hossain S, Hashimoto M, Katakura M, Al Mamun A, Shido O. Medicinal value of asiaticoside for Alzheimer's disease as assessed using single-molecule-detection fluorescence correlation spectroscopy, laser-scanning microscopy, transmission electron microscopy, and in silico docking. BMC Complement Altern Med 2015;15:118. https://doi.org/10.1186/s12906-015-0620-9

[36] Rajput MS, Nirmal NP, Rathore D, Dahima R. Dimethyl fumarate mitigates tauopathy in Aβ-induced neuroblastoma SH-SY5Y cells. Neurochem Res 2020;45(11):2641-2652. https://doi.org/10.1007/s11064-020-03115-x

[37] Baysal E, Zırh EB, Buber E, Jakobsen TK, Zeybek ND. The effect of melatonin on Hippo signaling pathway in dental pulp stem cells. Neurochem Int 2021;148:105079. https://doi.org/10.1016/j.neuint.2021.105079

[38] Tang Z, Cao J, Yao J, et al. KDM1A-mediated upregulation of METTL3 ameliorates Alzheimer's disease via enhancing autophagic clearance of p-Tau through m6A-dependent regulation of STUB1. Free Radic Biol Med 2023;195:343-358. https://doi.org/10.1016/j.freeradbiomed.2022.12.099

[39] Chonpathompikunlert P, Han J, Toh K, Isoda H, Nagasaki Y. TEMPOL protects human neuroblastoma SH-SY5Y cells against β-amyloid-induced cell toxicity. Eur J Pharmacol 2011;650(2-3):544-549. https://doi.org/10.1016/j.ejphar.2010.10.028

[40] Tarutani A, Suzuki G, Shimozawa A, et al. The effect of fragmented pathogenic α-synuclein seeds on prion-like propagation. J Biol Chem 2016;291(36):18675-18688. https://doi.org/10.1074/jbc.M116.734707

[41] Polinski NK, Volpicelli-Daley LA, Sortwell CE, et al. Best practices for generating and using alpha-synuclein pre-formed fibrils to model Parkinson's disease in rodents. J Parkinsons Dis 2018;8(2):303-322. https://doi.org/10.3233/JPD-171248

[42] Zhao N, Sun C, Zheng M, Liu S, Shi R. Amentoflavone suppresses amyloid β1-42 neurotoxicity in Alzheimer's disease through the inhibition of pyroptosis. Life Sci 2019;239:117043. https://doi.org/10.1016/j.lfs.2019.117043

[43] Celik Topkara K, Kilinc E, Cetinkaya A, Saylan A, Demir S. Therapeutic effects of carvacrol on beta-amyloid-induced impairments in in vitro and in vivo models of Alzheimer's disease. Eur J Neurosci 2022;56(9):5714-5726. https://doi.org/10.1111/ejn.15565

[44] Pathak R, Bhangu SK, Martin GJO, Separovic F, Ashokkumar M. Ultrasound-induced protein restructuring and ordered aggregation to form amyloid crystals. Eur Biophys J 2022;51(4-5):335-352. https://doi.org/10.1007/s00249-022-01601-4

[45] Asadi A, Pourfattah F, Miklós Szilágyi I, et al. Effect of sonication characteristics on stability, thermophysical properties, and heat transfer of nanofluids: A comprehensive review. Ultrason Sonochem 2019;58:104701. https://doi.org/10.1016/j.ultsonch.2019.104701

[46] Paravastu AK, Leapman RD, Yau WM, Tycko R. Molecular structural basis for polymorphism in Alzheimer's beta-amyloid fibrils. Proc Natl Acad Sci U S A 2008;105(47):18349-18354. https://doi.org/10.1073/pnas.0806270105

[47] Harry GJ, Billingsley M, Bruinink A, et al. In vitro techniques for the assessment of neurotoxicity. Environ Health Perspect 1998;106(Suppl 1):131-158. https://doi.org/10.1289/ehp.98106s1131

[48] Haugabook SJ, Yager DM, Eckman EA, Golde TE, Younkin SG, Eckman CB. High throughput screens for the identification of compounds that alter the accumulation of the Alzheimer's amyloid beta peptide (Abeta). J Neurosci Methods 2001;108(2):171-179. https://doi.org/10.1016/s0165-0270(01)00388-0

[49] Yahata N, Asai M, Kitaoka S, et al. Anti-Aβ drug screening platform using human iPS cell-derived neurons for the treatment of Alzheimer's disease. PLoS One 2011;6(9):e25788. https://doi.org/10.1371/journal.pone.0025788

[50] Wang X, Zhang R, Lin Y, Shi P. Inhibition of NF-κB might enhance the protective role of roflupram on SH-SY5Y cells under amyloid β stimulation via PI3K/AKT/mTOR signaling pathway. Int J Neurosci 2021;131(9):864-874. https://doi.org/10.1080/00207454.2020.1759588

[51] Song L, Yao L, Zhang L, Piao Z, Lu Y. Schizandrol A protects against Aβ1-42-induced autophagy via activation of PI3K/AKT/mTOR pathway in SH-SY5Y cells and primary hippocampal neurons. Naunyn Schmiedebergs Arch Pharmacol 2020;393(9):1739-1752. https://doi.org/10.1007/s00210-019-01792-2

[52] Çelik H, Karahan H, Kelicen-Uğur P. Effect of atorvastatin on Aβ1-42-induced alteration of SESN2, SIRT1, LC3II and TPP1 protein expressions in neuronal cell cultures. J Pharm Pharmacol 2020;72(3):424-436. https://doi.org/10.1111/jphp.13208

[53] Khan WU, Salman M, Ali M, et al. Neuroprotective effects of sulforaphane in a rat model of Alzheimer's disease induced by Aβ (1-42) peptides. Neurochem Int 2024;179:105839. https://doi.org/10.1016/j.neuint.2024.105839

[54] Ross A, Xing V, Wang TT, et al. Alleviating toxic α-Synuclein accumulation by membrane depolarization: evidence from an in vitro model of Parkinson's disease. Mol Brain 2020;13(1):108. https://doi.org/10.1186/s13041-020-00648-8

[55] Gao J, Perera G, Bhadbhade M, Halliday GM, Dzamko N. Autophagy activation promotes clearance of α-synuclein inclusions in fibril-seeded human neural cells. J Biol Chem 2019;294(39):14241-14256. https://doi.org/10.1074/jbc.RA119.008733